Measuring optical frequencies in the 0–40 THz range with non-synchronized electro–optic sampling

P. GAAL[1], M. B. RASCHKE[1,2], K. REIMANN[1]* AND M. WOERNER[1]

[1]Max-Born-Institut für Nichtlineare Optik und Kurzzeitspektroskopie, 12489 Berlin, Germany
[2]Department of Chemistry, University of Washington, Seattle, Washington 98195-1700, USA
*e-mail: reimann@mbi-berlin.de

Published online: 1 October 2007; doi:10.1038/nphoton.2007.170

Measurements using optical frequency combs[1–6] are now important in high-precision spectroscopy. However, measurement techniques described so far are either restricted to narrow frequency ranges or are difficult to implement in the far-infrared regime. Here we present a time-domain method for the direct measurement of optical frequencies in the mid- and far-infrared spectral region. The method is analogous to a sampling scope, with the electric field of the source measured by electro–optic sampling[7–13] using the light pulses from a femtosecond laser as a probe. The highest optical frequency that can be measured with our 'sampling scope' is determined by the pulse length of the femtosecond laser. When 12-fs probe pulses are used, a measurement of up to 40 THz, corresponding to a wavelength of 7.5 μm, is possible[9].

As the sampling rate, which is equal to the repetition rate $f_R = 1/T = 72$ MHz (where T is the time between two consecutive pulses) of the femtosecond laser, is much lower than the optical frequency ν to be determined (here $\nu = 28$ THz), it is not possible to determine $E(t)$ in real time. Typically in electro–optic sampling both the pulses to be measured and the probe pulses are derived from a common source, so that both pulses are synchronized; that is, $E(t) = E(t + T)$. This allows for measuring the complete electric-field transient by scanning the delay between both pulses and also for improving the signal-to-noise ratio by averaging over many pulses. In our case, however, we want to measure a source not synchronized to the probe pulses. In that case, averaging over consecutive probe pulses would yield zero signal, so the electro–optic signal has to be recorded for each pulse.

To demonstrate our method we investigate a continuous-wave (c.w.) CO_2 laser tuned to the 10P20 line with a wavelength of 10.591043 μm (this value is taken from the HITRAN database, see http://cfa-www.harvard.edu/HITRAN). Our source for the probe pulses is a Ti:sapphire oscillator yielding 12-fs pulses with a centre wavelength of 800 nm at a repetition rate of 72 MHz. A schematic of the experimental set-up is shown in Fig. 1 (for further details see Methods). The beams from the CO_2 laser and from the Ti:sapphire oscillator are combined at a beamsplitter and focused onto the electro–optic crystal, a ZnTe crystal. The electric field from the CO_2 laser induces birefringence in the electro–optic crystal, which is then probed by the femtosecond pulses and converted into an electric signal, proportional to the electric field.

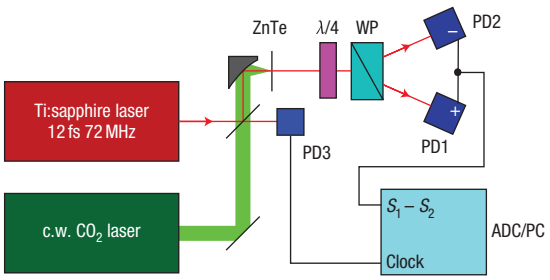

Figure 1 Schematic of the experimental set-up. The CO_2 laser is focused onto the ZnTe electro–optic crystal, where it induces birefringence. This birefringence is probed by 12-fs pulses from a Ti:sapphire laser, using the quarterwave plate (λ/4), the Wollaston polarizer (WP), and the two photodiodes PD1 and PD2. The difference signal from these two photodiodes is measured with a high-speed analog-to-digital converter (ADC) in a personal computer (PC), synchronized to the Ti:sapphire laser repetition rate with photodiode 3 (PD3).

The electric signal is fed into a high-speed analog-to-digital converter synchronized to the oscillator repetition rate. The signal is stored for every single probe pulse. The difference signal is subsequently normalized with respect to the sum of the signals from the two photodiodes (S_1 is the signal from photodiode 1, S_2 the signal from photodiode 2): $S = (S_1 - S_2)/(S_1 + S_2)$. A typical measurement consists of a set of 50 million values acquired within 0.7 s.

In Fig. 2 we see a short section of such a measurement. Figure 2a shows the noise of the electro–optic signal S when the CO_2 laser is blocked. Figure 2b shows S when the CO_2 is incident on the electro–optic crystal, that is, signal and noise. Although the average in both cases is equal to zero, one can see a difference in absolute values when the CO_2 laser is on with the root-mean-square (r.m.s.) value of the noise and of the signal alone both being 7×10^{-5}. The signal-to-noise ratio in a single shot is one. Shot noise is the dominant contribution as deduced from comparison with the expected value of 5×10^{-5} (see Methods). The r.m.s. electric field from the CO_2 laser at the position of the electro–optic crystal as calculated from the average power and the focus spot size is 1.5 kV cm^{-1}. Figure 2c shows the r.m.s.

© 2007 Nature Publishing Group

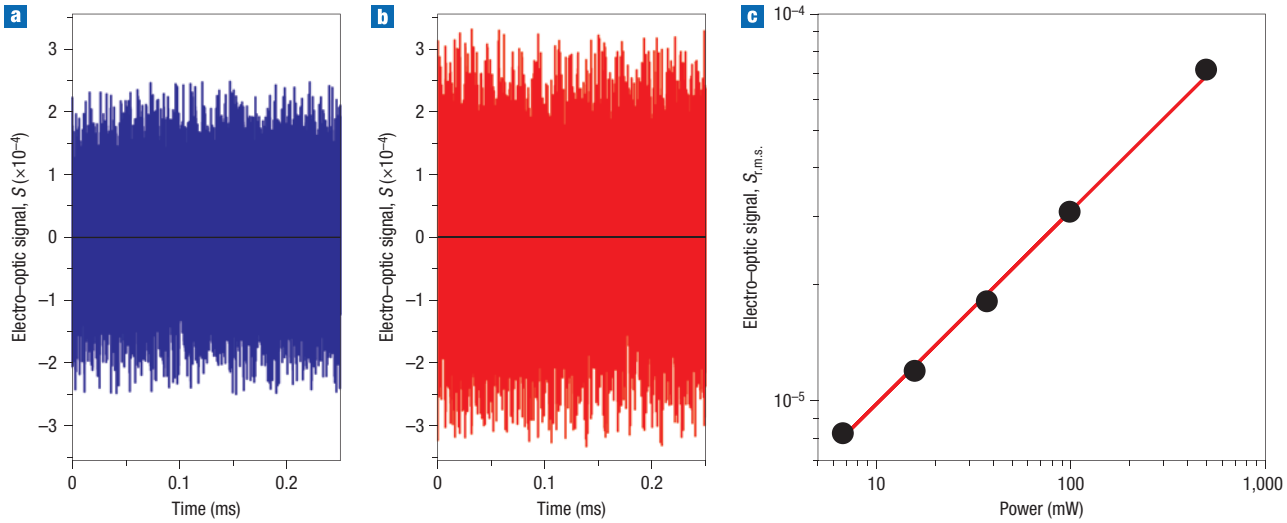

Figure 2 Experimental results for the electro–optic signal. a,**b**, Electro–optic signal measured without the CO_2 laser (**a**) and with the CO_2 laser (**b**). **c**, Dependence of the CO_2-laser-induced electro–optic signal $S_{r.m.s.}$ on incident power. $S_{r.m.s.}$ is defined as the square root of the difference between the average of the signal squared with the laser and the average of the signal squared without the laser. The dots are experimental results, and the line shows a square-root dependence.

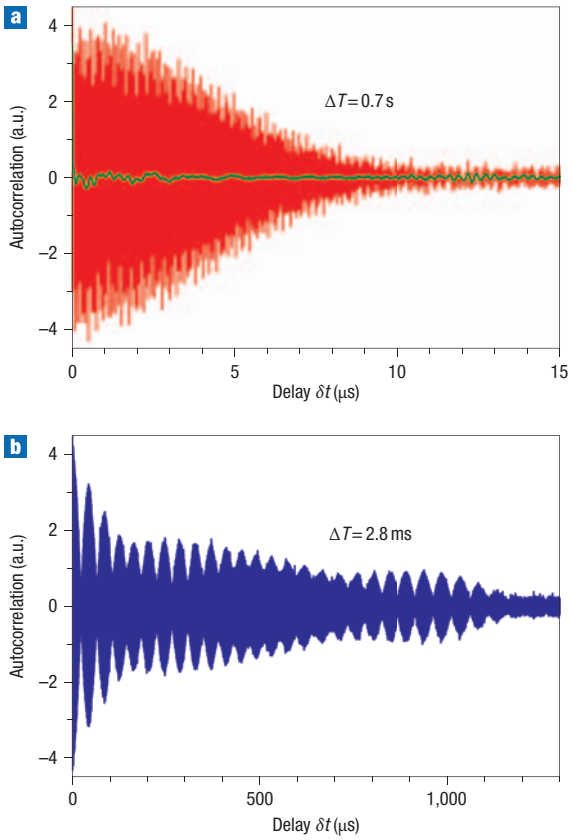

Figure 3 Autocorrelation of the electro–optic signal for different measurement times ΔT. a, Autocorrelation for a measurement time of $\Delta T = 0.7$ s with (red trace) and without (green line) the CO_2 laser. **b**, Autocorrelation for a measurement time of $\Delta T = 2.8$ ms with the CO_2 laser (blue trace). Note the different timescales in **a** and **b**. In all cases the peak at $\delta t = 0$ is outside the figure; in the units used it has a value of 9.8 with and 3.5 without the CO_2 laser.

value of the signal for different average powers. As expected, it is found that the signal, which is proportional to the amplitude of the electric field, increases as the square root of the CO_2 laser power (the solid line corresponds to a fit to the data with slope 0.5). Our sampling method may be an interesting alternative for measuring the time-resolved intensity of pulsed light sources in the mid- to far-infrared. The established technique for this purpose is upconversion with femtosecond gate pulses[14], which, however, becomes increasingly difficult for long wavelengths.

The data in Fig. 2a are random noise, and at first glance the data in Fig. 2b also look like random noise. That this is not the case can be seen from the autocorrelation of the data, which measures the amount of correlation between the data at two instants of time separated by the delay δt. The autocorrelation $A(\delta t)$ is defined as[15]

$$A(\delta t) = \frac{1}{N}\sum_{i=1}^{N} S(t_i) \times S(t_i + \delta t) \qquad (1)$$

Autocorrelations calculated from our data are shown in Fig. 3, both for a complete data set of $N = 5 \times 10^7$ points taken within a measurement time of $\Delta T = 0.7$ s (red trace in Fig. 3a) and for $N = 200{,}000$ and $\Delta T = 2.8$ ms (blue trace in Fig. 3b). For comparison, the autocorrelation of the noise is shown (green line in Fig. 3a). If the data were just random noise, $A(\delta t)$ would consist of only a single peak at $\delta t = 0$. The autocorrelations clearly show that the electro–optic signal obtained with the CO_2 laser is not random noise, but that there exists a correlation between the CO_2 laser electric-field values probed up to 10 μs (for $\Delta T = 0.7$ s) or even more than 1,000 μs (for $\Delta T = 2.8$ ms) apart. This shows that the CO_2 laser emits highly coherent radiation with coherence lengths of 1.5 km and 150 km, respectively.

The frequency of the electric field can be obtained from a Fourier transform[16] of the data. For $\Delta T = 0.7$ s one obtains the spectrum shown as the red line in Fig. 4, which shows a pronounced peak at a centre frequency of $f_C = 20.88$ MHz with a width of 90 kHz. As shown in the inset, the amplitude of this peak exceeds the noise level by six orders of magnitude, which

© 2007 Nature Publishing Group

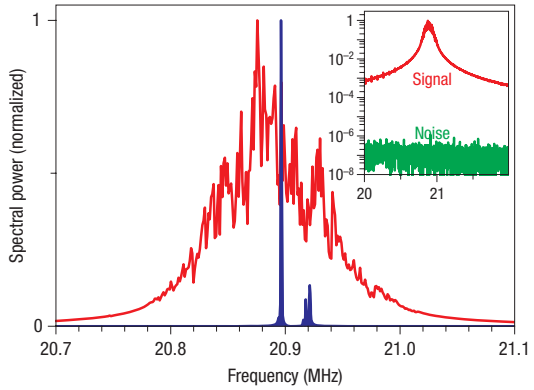

Figure 4 Spectra of the data. The red line shows the spectrum for a measurement time of $\Delta T = 0.7$ s, the blue line for $\Delta T = 2.8$ ms. The inset shows the data for $\Delta T = 0.7$ s again, together with the spectrum of the noise (green trace).

demonstrates that the peak at f_C can be measured even for average powers as low as a few microwatts.

Repeating the same measurement within several minutes, one obtains similar spectra, but the peak frequency varies within ± 2 MHz. This suggests that the linewidth is influenced by the variation of f_C within the measurement time ΔT. That this is indeed the case is shown by the blue line in Fig. 4, obtained by reducing the measurement time to 2.8 ms, which shows a linewidth of only 600 Hz. The small peak 25 kHz above the main peak in the spectrum (blue line in Fig. 4) corresponds to the beat note with a period of 40 μs observed in the autocorrelation (blue line in Fig. 3b).

The linewidth of the observed peak at f_C directly yields the linewidth of the electric field at the optical frequency ν. To obtain the optical frequency ν, we have to consider that the frequency of the signal is obtained by sampling an electric field oscillating with frequency ν with sampling rate f_R below the Nyquist limit[15] of 2ν. Here, the frequency f_C is given by $f_C = \min(f'_C, f_R - f'_C)$ with $f'_C = \nu \bmod f_R$. Inverting this equation, the optical frequency ν is given by

$$\nu = n \times f_R \pm f_C \quad (n \text{ is an integer}) \qquad (2)$$

Apart from the measured value of f_C, the determination of ν thus requires the knowledge of n and of the sign in equation (2). As is typical in high-precision spectroscopy, the frequencies to be measured are known beforehand with sufficient accuracy, so n and the sign of f_C are known. Alternatively, measurements with slightly different values for f_R have to be performed. In our case the maximum of the spectrum taken for $\Delta T = 0.7$ s (red line in Fig. 4) is at $f_C = 20.88$ MHz. As we know that the CO_2 laser operates on the 10P20 line, we find with $f_R = 71.586602$ MHz, $n = 395{,}401$ and the sign is positive in equation (2). This results in $\nu = 28{,}306{,}225.7$ MHz. The absolute accuracy of ν is presently limited by the accuracy of f_R (0.5 Hz) to 0.2 MHz (see Methods for a discussion of the achievable accuracy).

The main source for the linewidths measured are fluctuations of the length of the CO_2 laser resonator, of the Ti:sapphire laser resonator (see Methods), or of both. Although our study demonstrates the principle of a sampling scope for optical frequencies, for accurate determinations of optical frequencies ν and their linewidths, the Ti:sapphire laser repetition rate can be actively stabilized[4,17]. This is all the more important because an error in the value for the repetition rate of Δf_R results in an error of $n\Delta f_R$ for ν, where n can be very large, in particular in the mid-infrared. It would therefore also be advantageous to increase f_R, for example, to 1 GHz (ref. 18). This makes it easier to find the multiplier n (the free spectral range increases), and it softens the requirements for the accuracy of f_R.

The main advantage of our proposed scheme is that it is applicable to any frequency between 0 and 40 THz (the upper limit can be increased further by using shorter probe pulses). Other methods for frequency measurements in the mid- and far-infrared[4,5] either require the near coincidence of a known molecular transition with the frequency to be measured and are therefore limited to a narrow frequency range, or they use sum-frequency generation[6], which becomes difficult in the far-infrared. Another advantage is that no mid- or far-infrared detectors are needed.

METHODS

EXPERIMENTAL

The c.w. CO_2 laser we used was a linearly polarized, single-longitudinal-mode laser with an average power of 1 W (Lasy 4SL, Access Laser). It can operate on several lines in the 10P and 10R bands depending on its resonator length, which in turn depends on its temperature. Our Ti:sapphire oscillator was a Femtosource scientific from Femtolasers. Its repetition rate f_R was measured with the frequency counter Agilent 51131A-001. The beamsplitter was an undoped silicon plate under Brewster's angle, reflecting the *s*-polarized oscillator beam and transmitting the *p*-polarized CO_2 laser beam. For focusing we used a 90° off-axis parabolic mirror with a focal length of 12.7 mm. The electro–optic crystal was a 0.4-mm-thick (110) cut ZnTe crystal (because of tight focusing and because of the mismatch between the phase velocity of the mid-infrared and the group velocity of the femtosecond pulses, only ~10 μm of the ZnTe contribute to the signal). With a quarter-wave plate (denoted $\lambda/4$ in Fig. 1), a Wollaston polarizer (WP), and a pair of balanced photodiodes (AEPX65, Centronic, denoted PD1 and PD2 in Fig. 1), the polarization state of the electro–optic crystal, which is in turn determined by the electric field to be measured, was converted into a difference signal between the two photodiodes[11,19]. The high-speed analog-to-digital converter was a PCI-5122 (National Instruments), synchronized to the oscillator repetition rate using photodiode 3 (PD3).

FREQUENCY RANGE

We show here only results for one mid-infrared frequency, but the method of electro–optic sampling is applicable[7–9] for all frequencies between 0 and at least 40 THz, and there even exist measurements[12] at frequencies of more than 100 THz. For a given electro–optic crystal sensitivity depends on frequency[10]. In particular, sensitivity is typically quite low in the frequency range around the optical phonon frequency. One can, however, always choose a different electro–optic crystal with a different phonon frequency.

SHOT NOISE

Each of the two photodiodes receives only a finite number p of photons per pulse (at 15 mW average power per photodiode $p = 9 \times 10^8$), so the signal from every photodiode measured with a single probe pulse will have a relative shot-noise contribution according to Poisson statistics of $\sqrt{1/p} = 3 \times 10^{-5}$. Accordingly, the relative shot-noise contribution to the difference between the signals from the two photodiodes will be $\sqrt{2}$ as large; that is, $\Delta S = \sqrt{2/p} = 5 \times 10^{-5}$.

EFFECTS OF REPETITION-RATE DRIFTS AND OF PULSE-TO-PULSE JITTER

An ideal mode-locked laser will emit identical pulses equally spaced in time. Such an ideal laser would yield a frequency resolution equal to the inverse of the measurement time. All real lasers, however, differ in some respects from the ideal case. On the one hand, the emitted pulses are usually not identical. For many applications in metrology, their most important difference is in their carrier-envelope phase. However, we need not consider this carrier-envelope phase, as our signal depends only on the pulse envelope. Fluctuations of the pulse amplitude will lead to an additional noise contribution, in effect similar to the shot noise considered above. On the other hand, the demand 'equally spaced in time' is not strictly fulfilled in a real laser[20]. We have performed simulations of the effect of fluctuations of the repetition rate on our results. Such fluctuations

© 2007 Nature Publishing Group

can occur on all timescales. One extreme is a slow variation of the repetition rate f_R. If f_R varies linearly during a measurement by Δf_R, this leads to a linewidth of $n\Delta f_R$ for f_C and for ν. Assuming that the linewidths we observe are caused only by such slow variations of f_R, that is, that ν of the CO_2 laser is perfectly stable, we find in our measurements a frequency drift of ~ 0.3 Hz s^{-1}, which corresponds to a temperature drift of the laser of 0.2 mK s^{-1}. Such slow variations of the repetition rate can be compensated by control electronics. Very sophisticated techniques including locking to an atomic clock have resulted in relative changes of the repetition rate of less than 10^{-12} for a time of 1 s and even less for longer times[4,6]. With such a stabilized laser we could achieve a frequency resolution of less than 30 Hz for a measurement time of 1 s.

The other extreme is given by random fluctuations of the time between two consecutive pulses. Our simulations show that such rapid fluctuations do not broaden the observed lines, but only decrease their amplitude (the same effect is well known in X-ray crystallography as the Debye–Waller factor[21]), which becomes zero if the r.m.s. pulse-to-pulse fluctuations become as large as $(\sqrt{2\nu})^{-1}$, here 25 fs. We estimate that our pulse-to-pulse fluctuations are below 3 fs, which is similar to the 2 fs determined in ref. 20.

Received 24 April 2007; accepted 5 August 2007; published 1 October 2007.

References

1. Udem, T., Reichert, J., Holzwarth, R. & Hänsch, T. W. Absolute optical frequency measurement of the cesium D_1 line with a mode-locked laser. *Phys. Rev. Lett.* **82,** 3568–3571 (1999).
2. Hall, J. L. *et al.* Ultrasensitive spectroscopy, the ultrastable lasers, the ultrafast lasers, and the seriously nonlinear fiber: A new alliance for physics and metrology. *IEEE J. Quantum Electron.* **37,** 1482–1492 (2001).
3. Holzwarth, R., Zimmermann, M., Udem, T. & Hänsch, T. W. Optical clockworks and the measurement of laser frequencies with a mode-locked frequency comb. *IEEE J. Quantum Electron.* **37,** 1493–1501 (2001).
4. Amy-Klein, A. *et al.* Absolute frequency measurement in the 28-THz spectral region with a femtosecond laser comb and a long-distance optical link to a primary standard. *Appl. Phys. B* **78,** 25–30 (2004).
5. Siemsen, K. J. & Bernard, J. E. A phase-sensitive technique to measure small changes in laser frequency: Application to measure the shift and broadening of a saturated absorption line of OsO_4. *Appl. Phys. B* **81,** 497–502 (2005).
6. Amy-Klein, A. *et al.* Absolute frequency measurement of a SF_6 two-photon line by use of a femtosecond optical comb and sum-frequency generation. *Opt. Lett.* **30,** 3320–3322 (2005).
7. Wu, Q. & Zhang, X.-C. Free-space electro-optic sampling of terahertz beams. *Appl. Phys. Lett.* **67,** 3523–3525 (1995).
8. Wu, Q. & Zhang, X.-C. Free-space electro-optics sampling of mid-infrared pulses. *Appl. Phys. Lett.* **71,** 1285–1286 (1997).
9. Huber, R., Brodschelm, A., Tauser, F. & Leitenstorfer, A. Generation and field-resolved detection of femtosecond electromagnetic pulses tunable up to 41 THz. *Appl. Phys. Lett.* **76,** 3191–3193 (2000).
10. Leitenstorfer, A., Hunsche, S., Shah, J., Nuss, M. C. & Knox, W. H. Detectors and sources for ultrabroadband electro-optic sampling: Experiment and theory. *Appl. Phys. Lett.* **74,** 1516–1518 (1999).
11. Reimann, K., Smith, R. P., Weiner, A. M., Elsaesser, T. & Woerner, M. Direct field-resolved detection of terahertz transients with amplitudes of megavolts per centimeter. *Opt. Lett.* **28,** 471–473 (2003).
12. Kübler, C., Huber, R., Tübel, S. & Leitenstorfer, A. Ultrabroadband detection of multi-terahertz field transients with GaSe electro-optic sensors: Approaching the near infrared. *Appl. Phys. Lett.* **85,** 3360–3362 (2004).
13. Bartel, T., Gaal, P., Reimann, K., Woerner, M. & Elsaesser, T. Generation of single-cycle THz transients with high electric-field amplitudes. *Opt. Lett.* **30,** 2805–2807 (2005).
14. Kaindl, R. A. *et al.* Homogeneous broadening and excitation-induced dephasing of intersubband transitions in a quasi-two-dimensional electron gas. *Phys. Rev. B* **63,** 161308(R) (2001).
15. Press, W. H., Flannery, B. P., Teukolsky, S. A. & Vetterling, W. T. *Numerical Recipes* (Cambridge Univ. Press, Cambridge, 1986).
16. Frigo, M. & Johnson, S. G. The design and implementation of FFTW3. *Proc. IEEE* **93,** 216–231 (2005).
17. Ramond, T. M., Diddams, S. A., Hollberg, L. & Bartels, A. Phase-coherent link from optical to microwave frequencies by means of the broadband continuum from a 1-GHz Ti:sapphire femtosecond oscillator. *Opt. Lett.* **27,** 1842–1844 (2002).
18. Bartels, A. & Kurz, H. Generation of a broadband continuum by a Ti:sapphire femtosecond oscillator with a 1-GHz repetition rate. *Opt. Lett.* **27,** 1839–1841 (2002).
19. Planken, P. C. M., Nienhuys, H.-K., Bakker, H. J. & Wenckebach, T. Measurement and calculation of the orientation dependence of terahertz pulse detection in ZnTe. *J. Opt. Soc. Am. B* **18,** 313–317 (2001).
20. Leitenstorfer, A., Fürst, C. & Laubereau, A. Widely tunable two-color mode-locked Ti:sapphire laser with pulse jitter of less than 2 fs. *Opt. Lett.* **20,** 916–918 (1995).
21. Waller, I. Zur Frage der Einwirkung der Wärmebewegung auf die Interferenz von Röntgenstrahlen. *Z. Phys.* **17,** 398–408 (1923).

Acknowledgements

The authors acknowledge financial support by the Deutsche Forschungsgemeinschaft.
Correspondence and requests for materials should be addressed to K.R.

Reprints and permission information is available online at http://npg.nature.com/reprintsandpermissions/

© 2007 Nature Publishing Group